Memetic Improved Cuckoo Search Algorithm for Automatic B-spline Border Detection of Cutaneous Melanoma From Macroscopic Medical Images

Akemi Gálvez, Andrés Iglesias

Abstract

This work follows up a previous paper at conference Cyberworlds 2018 for automatic border detection of cutaneous melanoma and other skin lesions from macroscopic medical images. Given a set of feature points on the boundary of the skin lesion obtained by a dermatologist, we introduce a new method for automatic least-squares B-spline curve fitting of such feature points. The method is based on the original cuckoo search algorithm used in the conference paper but with three major modifications: (1) we use an enhanced version of the algorithm in which the parameters change dynamically with the generations; (2) this improved method is coupled with the Luus-Jaakola local search heuristics for better performance; (3) the original Bézier curves are now replaced by the more powerful and more general B-spline curves, providing extra flexibility and lower polynomial degree. The new method (called *memetic improved cuckoo search algorithm*) has been applied to a benchmark comprised of ten medical images of skin lesions. The computer results show that it performs very well and yields a border curve enclosing the lesion and fitting the feature points with good accuracy. Furthermore, a comparison with ten alternative methods in the literature (six standard mathematical methods for B-spline fitting, two state-of-the art methods in medical imaging, the method in our conference paper and the non-memetic version of our new method) shows that it outperforms all these methods in terms of numerical accuracy for the instances in our reference benchmark.

Keywords: swarm intelligence, cuckoo search algorithm, medical image segmentation, cutaneous melanoma, border detection, B-spline curves

1. Introduction

1.1. Motivation

Malignant cutaneous melanoma is the most common type of skin cancer. According to figures of the World Health Organization, the number of patients in 2015 was more than 3.1 million people worldwide, with about 60,000 deceases. It is a particularly dangerous cancer because it can invade nearby tissues and spread to other parts of the body (e.g., liver, bone, lung, or brain). It is also one of the most rapidly increasing kinds of cancer in the world. Just for illustration, a total of more than 68,100 cases and 8,700 deceases were reported in USA in 2010. These figures escalated to more

than 73,800 cases and 9,900 deceases in 2015 and last available data suggest that this increasing tendency will continue for a while. As a result, melanoma has become one of the biggest current concerns all over the world regarding public health.

Melanoma is a kind of cancer typically caused by the ultraviolet light exposure (although other factors can also play an important role in many cases). It arises from pigment-containing cells called *melanocytes*. As such, it usually happens in the skin (then called *cutaneous melanoma*) although cases of melanoma have also been reported in the mouth, digestive tract, and even the eye. However, those cases are quite rare, so melanoma is usually considered to be a skin disease. A very important feature of melanoma is that early detection is critical for survival. When detected early, the 5-year survival rate ranges between 89∼95% for stages I and II with peaks of 99% for stage 0, while it decreases to 25∼70% for stage III and only 7∼20% for stage IV. In this regard, early diagnosis is particularly important as early-stage melanoma can usually be removed by a simple clinical procedure (very often, just a simple excision might be enough).

Visual inspection by self-examination or examination by a specialist are the most usual diagnostic procedures. Unfortunately, it is often hard to discriminate the melanoma from other skin diseases such as common moles or naevus. Therefore, this procedure is subjective and time-consuming, even for trained practitioners. Other diagnostic procedures include the popular ABCDE (Asymmetry, Border irregular, Color uneven, Diameter, Evolving) method, the 7-point checklist, the Menzies scale, and some types of biopsy (tangential, incisional, punch, excisional, optical, etc). However, since these procedures rely strongly on human intervention, they can lead to medical results that can differ even among experienced dermatologists. Other kind of procedures involve imaging tests, such as X-ray, computer tomography (CT) scan, positron emission tomography (PET) scan, magnetic resonance imaging (MRI) scan, and others. In most cases, these procedures are used to look for the possible spread of melanoma to lymph nodes or other organs in the body rather than for early identification.

Two commonly used image acquisition methods for early diagnosis are standard digital camera and dermoscopy. The former is of great help for patients with difficult access to a dermatologist, as they can simply take a close picture with a standard digital camera or mobile phone (macroscopic image) and send it to the professional for remote examination. Dermoscopy is more precise and improves the discrimination between a real cutaneous melanoma and other skin lesions. As a consequence, it is very useful for decreasing the cases of screening errors [3]. However, it is also affected by errors derived from the subjectivity of human interpretation of images, and it is therefore dependent on the proficiency of the medical expert. In fact, it has been shown that the accuracy of early diagnosis decreases significantly for inexperienced practitioners.

The previous discussion emphasizes the need for computer-aided techniques for automatic diagnosis of melanoma at early stages. Although some semi-automatic methods for early diagnosis have already been developed, they still rely on human intervention and therefore, they are error-prone and time-consuming. Nowadays, there is a strong demand for automated procedures at least to alleviate the load on the human part in some critical steps (semi-automatic diagnosis). This is a top priority in current research

in the field and the main motivation of this paper.

1.2. Segmentation procedures

The first goal in melanoma diagnosis is to classify the skin lesion as benign or malignant. To this aim, automatic or semi-automatic analysis of medical images is commonly used in a diagnosis pipeline involving several steps. One of the most important ones is *image segmentation*. At this step, the lesion is roughly discriminated from the background skin to focus on the area of interest for better identification and classification of the melanoma. Several methods have been applied to this problem. Early popular imaging approaches focused on properties such as color, histogram or gradient. They include thresholding [6, 20], clustering [38, 49], and edge-based methods [2]. Other methods are: level set methods [32], gradient vector flow snakes [10, 50], and active contours [31], driven by the seminal work in computer graphics in [27].

The first task in segmentation is border detection, which means determining the border curve of the lesion from the image. This border structure is a useful source of helpful information for accurate diagnosis. For instance, usual clinical features for diagnosis, such as the asymmetry, border irregularity, or diameter (features tracked in the ABCDE method), can be seamlessly computed from the detected border. This boundary is also used for other important clinical procedures such as the extraction of blue-white areas, or the recognition of atypical pigment networks and globules, among others.

Until recently, the task of border detection was carried out manually by dermatologists. Based on their previous experience, they use the mouse to select different points of the picture on the computer screen to provide an input collection of feature points. Such points are joined with segments to define a draft polyline that must cover the full region of the skin lesion, either accurately in simple cases or in excess otherwise (so that the initial polyline will always be moved inward until it reaches the boundary of the skin lesion). Once again, this manual procedure is prone to errors and time consuming. It also demands a high degree of expertise for accurate results. Taking advantage of the segmentation methods mentioned above, it is desirable to automate the process for efficiency and higher accuracy. On the other hand, the polyline is not the best graphical primitive for this process, because the border of skin lesions is rarely piecewise linear, but smooth. Since the input data consists of a collection of 2D points, parametric approximation schemes seem to be particularly suitable for this task.

A previous paper by the authors presented at Cyberworlds 2018 conference [19] addressed this problem by using polynomial Bézier curves. In that case, we had to deal with a data parameterization problem, subsequently converted into a least-squares minimization problem. To solve it, a cuckoo search algorithm was proposed. The method was successful applied to compute the outline curves of two illustrative examples of a benign and a malignant skin lesions (a naevus and a melanoma, respectively).

In spite of our positive results, during the reviewing process it was pointed out that the complex shape of the boundaries of skin lesions typically demands very high degrees for data fitting through a single Bézier curve. Following the reviewer suggestions, the present paper overcomes this limitation by using piecewise polynomial functions,

particularly B-spline curves. Although these curves are more powerful than the Bézier counterpart, they are also more difficult to deal with, as they introduce new parameters (the breakpoints) that are also to be computed. To cope with these new extra parameters, our previous approach is modified in this paper in two different ways: on one hand, we consider a modification of the original cuckoo search algorithm that allows its parameters to change over the iterations instead of keeping a fixed value. On the other hand, the modified method is also coupled with a local search procedure to improve its performance. These new features are described in detail in Sect. 4.

1.3. Main contributions of this paper

Main contributions of this paper are:

- The previous approach in [19] based on Bézier curves is now replaced by the (more powerful) B-spline curves. The piecewise mathematical structure of the B-splines make them an ideal solution to overcome the problem of high polynomial degrees inherent in Bézier-based approximation schemes. The new approach is also more general, as the Bézier curves are particular cases of B-spline curves.

- Since the B-spline curves introduce new parameters (the breakpoints) that have also to be computed, the corresponding optimization problem becomes more difficult to solve. This new problem is now addressed by using a modification of the original cuckoo search algorithm called *improved cuckoo search algorithm* [41], which allows its parameters p_a and α to change over the iterations, instead of the fixed value used in the original algorithm. This modification leads to substantial improvements in computer speed and accuracy.

- This modified method is also hybridized with a local search optimizer called *Luus-Jaakola heuristics* to enhance the search capabilities of the method in the neighborhood of the local minima. Our results show that this memetic method leads to significant improvements in accuracy compared to the non-coupled version.

1.4. Structure of this paper

This paper is organized as follows: Section 2 describes some previous work on curve approximation, including the recent application of computational intelligence techniques for that purpose. The original cuckoo search algorithm, its improved version and its hybridization with the Luus-Jaakola heuristics for local search are described in Section 3. Our automatic method for border detection with B-spline curves is described in Section 4, including parameter tuning and implementation issues. Our experimental results on a benchmark of medical images of skin lesions is discussed in Section 5. Comparative work with other classical and state-of-the-art alternative methods in the field is also discussed in the section. The paper closes with the main conclusions and some plans for future work in the subject.

2. Previous Work

Data approximation with free-form curves has been a recurrent topic of research for several decades. Classical approaches based on numerical methods were introduced in the 60s and 70s, while more sophisticated methods were developed in the 80s and 90s to solve particular cases (see [5, 8, 11] for an introduction to the field). From a mathematical standpoint, the problem can be expressed as an optimization problem [8, 26]. Unfortunately, classical optimization techniques have not been very successful in solving the general problem, so several alternative methods have been proposed. They include curvature-based distance minimization [42], error bounds [34], and dominant points [35]. Although they are successful in solving academic cases, they are also limited by some ideal constraints (high differentiability, noiseless data) difficult to meet for many real-world instances.

In the last two decades some artificial intelligence methods have been proposed for this problem: standard neural networks [21], self-organizing maps [22], Bernstein basis function networks [29], and neural networks combined with partial differential equations [4]. The use of the more general functional networks is proposed in [24]. The paper in [25] applies support vector machines (SVM) to the least-squares fitting problem with B-spline curves. The work in [17] combines functional networks and genetic algorithms to enhance the performance.

The most recent trend in this area is to apply nature-inspired metaheuristic techniques [43, 44], such as those from evolutionary computation [7, 23] and swarm intelligence [9, 28]. Such techniques are very advantageous because they do not require the function under optimization to be differentiable, can be applied when little information is available, and are very robust to irregular or incomplete sampling, noise in data, and other artifacts. Evolutionary computation and swarm intelligence methods applied to this issue include genetic algorithms [47, 48] artificial immune systems [16, 40], particle swarm optimization [12], firefly algorithm [13, 14] and memetic approaches [15]. However, these schemes are generally tailored for explicit curves and cannot be applied to the parametric case. A recent paper by the authors filled this gap with a method based on cuckoo search for border detection with Bézier curves. The method works well, but requires high-degree curves for complex boundary shapes. In this work we aim at overcoming this limitation by means of a powerful modification of a nature-inspired method called cuckoo search algorithm to address the problem using B-spline curves, as discussed in next sections.

3. Cuckoo Search Algorithms

3.1. Original Method (CSA)

Cuckoo search algorithm (CSA) is a nature-inspired continuous optimization method proposed by X.S. Yang and S. Deb in 2009 [45]. The algorithm is based on the brood parasitism behavior by some cuckoo species that lay their eggs in the nests of other (host) birds. This strategy is aimed at avoiding the parental investment in the upbringing of their offspring, and to minimize the risk of egg loss by distributing the eggs

among several nests. Sometimes, it may happen that these host birds discover such alien eggs and take responsive actions (for instance: leaving the nest to build a new one or throwing the eggs away). At their turn, the brood parasites have also designed sophisticated strategies (i.e., shorter incubation periods for their eggs, a different egg coloration and even egg pattern mimicking those of the hosts, rapid nestling growth an others) to secure that the host birds will eventually take care of their progeny.

This unconventional behavior is used as a the metaphor for the cuckoo search algorithm. In CSA, the eggs in the nest represent a set of candidate solutions for an optimization problem with the cuckoo egg being a new candidate solution. The rationale of the method is to use these new solutions given by the cuckoo eggs to replace current solutions associated with by the eggs in the nest. This substitution, performed iteratively, will finally lead to a high-quality solutions of the problem.

For the computational implementation of the CSA, it is convenient to consider these three ideal rules [45, 46]:

1. Each cuckoo dumps one egg at each time, laid in a random nest;
2. At each generation, the best nests (associated with good solutions) will be maintained for next generation;
3. The number of host nests is considered fixed. Also, a host may discover an alien egg with a certain probability, $p_a \in [0, 1]$. Then, the host bird can throw the egg away or leave the nest to build another somewhere else.

For computational efficiency, the last rule can be replaced by an amount of the total nests being substituted by new ones. Also, for some optimization problems, the quality of a solution can be taken to be proportional to the fitness function. However, other sophisticated formulas for the objective function can be considered as well.

These basic rules are the core of the CSA. The main steps of its corresponding pseudocode are summarized in Table 1. We consider an initial population chosen randomly of n host nests and run the algorithm in an iterative fashion. In [45] the initial values of the jth component of the ith nest are given by $x_i^j(0) = rand.(up_i^j - low_i^j) + low_i^j$, with up_i^j and low_i^j being the upper and lower bounds of such a component, respectively, and $rand$ is a uniform random constant on the open interval $(0, 1)$. With this choice, the initial variable values of the variables are always inside the search space. These border conditions are systematically checked for each generation.

At each generation g, we select randomly a cuckoo egg i. Then, new solutions $\mathbf{x}_i(g+1)$ are generated through Lévy flights, a random walk approach where the steps are described by their step-lengths according to a probability distribution and whose directions are random and isotropic. As indicated in [45], the use of Lévy flights is adviced over other random walks as it provides better overall performance for the algorithm. The evolution equation for Lévy flights is as follows:

$$\mathbf{x}_i(g+1) = \mathbf{x}_i(g) + \alpha \oplus levy(\lambda) \tag{1}$$

where g means the current generation, $\alpha > 0$ is the step size (associated with the scale of the optimization problem) and symbol $\oplus$ means the entry-wise multiplication. We

Table 1: Original CSA with Lévy flights.

Algorithm: Original CSA via Lévy Flights

begin
Fitness function $h(\mathbf{x})$, $\mathbf{x} = (x_1, \ldots, x_D)^T$
Generate initial population of $\mathcal{P}$ host nests $\mathbf{x}_i$ $(i = 1, 2, \ldots, \mathcal{P})$
while $(t < MaxGeneration)$
Choose a cuckoo (say, i) randomly using Lévy flights
Computer its fitness, F_i
Select a new nest (say, j) randomly
if $(h(\mathbf{x}_i) > h(\mathbf{x}_j))$
Replace $\mathbf{x}_j$ by $\mathbf{x}_i$
end
An amount (p_a) of poor nests are abandoned; new
nests are built using Lévy flights
Preserve the best solutions (elitism)
Rank all solutions to determine the best one
end while
Return the best solution and fitness value
end

remark that Eq. (1) is basically a Markov chain, as the location at generation $g + 1$ only depends on the location at generation g (first term) and a transition probability (second term), modulated by the Lévy distribution as:

$$levy(\lambda) \sim g^{-\lambda}, \qquad (1 < \lambda \leqslant 3) \tag{2}$$

with infinite variance and infinite mean. Computationally, random numbers generation with Lévy flights is a two-step process: first, choose a random direction given by the uniform distribution; then, generate of steps according to the Lévy distribution. It is suggested to use the Mantegna algorithm for symmetric distributions, in which positive and negative steps are considered. The procedure is similar to that in our previous paper in [19], so the interested reader is kindly referred to that entry for further details.

At each generation, the cuckoo search algorithm computes the fitness of any new solution and compares it with the current one. In case of improvement, the new solution replaces the previous one. Also, all current solutions at that generation are ranked according to their fitness values and the best solution so far is stored in vector $\mathbf{x}_{best}$, which is then transferred to the next generation. Also, an amount of the worse nests is rejected and replaced by new candidate solutions to increase the explorative capabilities of the method to find better solutions. The ratio of replacement p_a is a

parameter of the method that requires proper tuning for optimal performance. This process is repeated for successive generations until a stopping criterion is met. Popular stopping criteria are: (1) reaching a solution better than a feasible threshold; (2) a given number of generations is reached, or (3) several back to back generations do not improve the results.

3.2. Improved Cuckoo Search Algorithm (ICSA)

The *improved cuckoo search algorithm* (ICSA) is a modification of the original CSA proposed in [41] for performance enhancement. In this modified version, the parameters p_a and α change dynamically over the time, in contrast with the fixed values in the original CSA. In ICSA the parameter p_a varies as:

$$p_a^t = p_{a_M} - \frac{p_{a_M} - p_{a_m}}{\Lambda}\, t \tag{3}$$

where M and m indicate the maximum and minimum values for the parameter respectively, and Λ means the total number of generations. According to Eq. (3), p_a decreases linearly with the generations from p_{a_M} to p_{a_m}. At initial stages, it takes a high value to promote diversity in the pool of solutions, but it is decreased at later stages to intensify the search in the neighborhood of best candidates of the population. The parameter α, taken constant in the CSA, is also used to promote a trade-off between exploration and exploitation in search space. In particular, it is varied dynamically as:

$$\alpha^t = \alpha_M\, Exp\left(\frac{Ln\left(\alpha_m/\alpha_M\right)}{\Lambda}\, t\right) \tag{4}$$

starting with a high value, α_M, for extensive exploration and reducing it to a low value, α_m, to enforce exploitation until reaching the optimum.

3.3. Memetic ICSA with Luus-Jaakola Heuristics

The success of nature-inspired metaheuristic techniques for optimization relies to a large extent on a feasible trade-off between two conflicting search procedures: exploration and exploitation. The former aims at generating solutions as varied as possible to move in the search space on a global scale. Exploitation focuses the search on a local region around a current good solution. An effective way to achieve this desired trade-off is given by the *memetic algorithms*, which consists of the hybridization of a global search optimization method with local search procedures [18]. This memetic paradigm is becoming popular owing to its adequate combination of global and local search features within a common framework.

In this paper, we present a new memetic approach for proper balance between exploration and exploitation. Our approach is based on the ICSA for global optimization described in Section 3.2. This modified improved scheme is coupled with a local search procedure: the *Luus-Jaakola* (LJ) method, introduced in [30] for nonlinear programming problems. It is a gradient-free heuristics with an initialization step, at which random uniform values are chosen within the search space. Then, the current position

of the potential solution is perturbed by adding a sampled random uniform value to each component within its lower and upper bounds to generate a new candidate solution. Whenever the fitness improves with this change, the new solution replaces the current one; otherwise, the sampling space is decreased by a multiplicative factor (taken as 0.98 in this work). This process is repeated iteratively such that the neighborhood of the solution decreases and the procedure finally converges to a point.

4. The Proposed Method

4.1. Problem to be Solved

The problem of *automatic border detection with B-spline curves* addressed here can be stated as follows:

> *Given a collection of feature points from the border of a skin lesion, determined by a trained dermatologist from a macroscopic image of the lesion, compute automatically the B-spline curve providing the best fitting (according to an error metrics) to the input data points and enclosing the lesion.*

If data were acquired from smooth and simple shapes through accurate procedures, the problem might be addressed through classical interpolation techniques. However, manually-acquired medical data are prone by noise and irregular sampling, so interpolation methods are not adequate, since they force the fitting functions to pass through the noisy outliers. To overcome this drawback, approximation techniques are applied instead. In this case, the border detection can be formulated as a continuous optimization problem in the form of a least-squares fitting problem [8, 36, 37].

An adequate choice of the fitting functions is required to solve this optimization problem. The best ones in this regard are the free-form parametric curves, which are very flexible and well-suited for interactive design. In our previous conference paper [19] we used Bézier curves, as they are simple to implement and very popular in many fields. However, during the review of the paper it was wisely remarked that fitting a large collection of data points through a single Bézier curve typically leads to very high degree polynomials for complicated and highly oscillating shapes, an undesirable feature in data fitting. The reviewer also suggested to employ piecewise polynomials instead. Several options are available for this task (e.g., cubic splines). Amongst them, the B-spline curves are the most preferred fitting curves, as they are very general and powerful and are included as basic primitives in all major CAD/CAM programs of the market. Based on these reasons, in this work we address the border detection problem with B-splines curves. These curves are described in next paragraphs. Further details can be found in [37].

Let $\boldsymbol{\Upsilon} = \{\upsilon_0 = \alpha, \upsilon_1, \ldots, \upsilon_\nu, \upsilon_{\nu+1} = \beta\}$ be a strictly increasing sequence of non-negative real numbers called *breakpoints* on the interval $[\alpha, \beta] \subset \mathbb{R}$. In this work vectors are written in bold. Without loss of generality, $[\alpha, \beta]$ can be $[0, 1]$. For each sequence $\boldsymbol{\Upsilon}$, the *k-th B-spline basis function* $\psi_k^\rho(\omega)$ *of order* ρ (i.e., degree $\rho - 1$) is

computed recurrently as:

$$\psi_k^1(\omega, \boldsymbol{\Upsilon}) = \begin{cases} 1 & \text{if } \upsilon_k \leqslant \omega < \upsilon_{k+1} \\ \\ 0 & \text{otherwise} \end{cases} \tag{5}$$

for $k = 0, \ldots, \nu$, and:

$$\psi_k^\rho(\omega, \boldsymbol{\Upsilon}) = \frac{\omega - \upsilon_k}{\upsilon_{k+\rho-1} - \upsilon_k} \psi_k^{\rho-1}(\omega, \boldsymbol{\Upsilon}) + \frac{\upsilon_{k+\rho} - \omega}{\upsilon_{k+\rho} - \upsilon_k} \psi_{k+1}^{\rho-1}(\omega, \boldsymbol{\Upsilon}) \tag{6}$$

for $\rho > 1$ and $k = 0, \ldots, \nu - \rho + 1$. When necessary, take $\frac{0}{0} = 0$ in Eq. (6). Note that $\psi_k^\rho(\omega, \boldsymbol{\Upsilon})$ is a nonlinear function of $\boldsymbol{\Upsilon}$.

A *B-spline curve of order ρ with breakpoints* $\boldsymbol{\Upsilon}$, denoted as $\boldsymbol{\Phi}(\omega, \boldsymbol{\Upsilon})$, is given by:

$$\boldsymbol{\Phi}(\omega, \boldsymbol{\Upsilon}) = \sum_{i=0}^{\sigma} \boldsymbol{\Xi}_i \, \psi_i^\rho(\omega, \boldsymbol{\Upsilon}) \tag{7}$$

where $\boldsymbol{\Xi} = \{\boldsymbol{\Xi}_i\}_{i=0,\ldots,\sigma}$ are coefficients of the curve called *poles* and $\{\psi_i^\rho(\omega, \boldsymbol{\Upsilon})\}_i$ are defined above. We assume that the end breakpoints are repeated ρ times, so that the curve interpolates the first and last poles, i.e., $\boldsymbol{\Phi}(\alpha, \boldsymbol{\Upsilon}) = \boldsymbol{\Xi}_0$ and $\boldsymbol{\Phi}(\beta, \boldsymbol{\Upsilon}) = \boldsymbol{\Xi}_\sigma$, a useful property in medical imaging applications and other fields. However, our method does not depend on these assumptions.

Consider now an input set of sorted featured points $\{\boldsymbol{\Theta}_k\}_{k=1,\ldots,\chi}$ on the boundary between a skin lesion and its background image, selected by a trained dermatologist from macroscopic images. Our goal is to determine the B-spline curve $\boldsymbol{\Phi}(\omega, \boldsymbol{\Upsilon})$ of order ρ approximating better such feature points $\{\boldsymbol{\Theta}_k\}_k$. Since the curve is parametric, we need a suitable data parameterization, so that each $\boldsymbol{\Theta}_k$ is associated with a parameter value $\xi_k \in [\alpha, \beta]$. According to our previous assumptions, we can take $\boldsymbol{\Phi}(\xi_1, \boldsymbol{\Upsilon}) = \boldsymbol{\Theta}_1$ and $\boldsymbol{\Phi}(\xi_\chi, \boldsymbol{\Upsilon}) = \boldsymbol{\Theta}_\chi$ and perform curve fitting on the remaining parameters:

$$\boldsymbol{\Theta}_k \approx \boldsymbol{\Phi}(\xi_k, \boldsymbol{\Upsilon}) = \sum_{i=0}^{\sigma} \boldsymbol{\Xi}_i \, \psi_i^\rho(\xi_k, \boldsymbol{\Upsilon}) \tag{8}$$

for $k = 2, \ldots, \chi - 1$. Eq. (8) can be compacted in matrix notation as:

$$\boldsymbol{\Theta} = \boldsymbol{\Psi}.\boldsymbol{\Xi} \tag{9}$$

where $\boldsymbol{\Theta} = (\boldsymbol{\Theta}_2, \ldots, \boldsymbol{\Theta}_{\chi-1})^T$, $\boldsymbol{\Xi} = (\boldsymbol{\Xi}_0, \ldots, \boldsymbol{\Xi}_\sigma)^T$, $\boldsymbol{\Psi} = \Big(\{\psi_i^\rho(\xi_l, \boldsymbol{\Upsilon})\}_{i=0,\ldots,\sigma\,;\, l=2,\ldots,\chi-1}\Big)$, and $(.)^T$ indicates the transpose of a matrix. Note that the dimension of the search space is given by $D \subset \mathbb{R}^n$ in Eq. (9) is $n(\sigma + 1) + \nu + \chi - 2$, which can be very large for complicated shapes.

The system (9) is overdetermined, so matrix $\mathbf{\Psi}$ is not invertible and the system has not analytical solution. Instead, we consider the least squares fitting of (8), given by:

$$\Lambda = \underset{\substack{\{\Xi_i\}_i \\ \{\upsilon_j\}_j \\ \{\xi_k\}_k}}{\text{minimize}} \left(\sum_{k=2}^{\chi-1} \left|\left| \mathbf{\Theta}_k - \sum_{i=0}^{\sigma} \Xi_i \, \psi_i^{\rho}(\xi_k, \mathbf{\Upsilon}) \right|\right|_2 \right) \tag{10}$$

where $||.||_2$ is the Euclidean norm. Since our input consists of the feature points exclusively, solving Eq. (10) requires to obtain *all* free variables of the problem. This is a difficult and challenging task, since such variables are intertwined in a complicated (and highly nonlinear) way. For this reason, many previous methods assume the values for some of those variables and then compute the remaining ones. As a result, the procedure depends on the initial choice of such values. Furthermore, the problem is nonconvex because the curve is a nonconvex function of the breakpoints, and multimodal (there could be several local minima of the fitness function). In short, Eq. (10) is a *nonlinear, multimodal, and nonconvex continuous optimization problem.*

4.2. Our Approach

Our procedure to solve the border detection problem is to apply the memetic ICSA described above to determine optimal values for the parameters of the functional Λ in Eq. (10). The input of our method consists of:

1. the input feature points, $\{\mathbf{\Theta}_k\}_{k=1,\ldots,\chi}$,
2. the order ρ of the B-spline curve, and
3. the number of poles, σ.

The first item is given by the dermatologist, while the last two items are chosen by the user. Regarding the order, low values provide little flexibility for shape control while high values introduce unwanted wriggles and require further computation, so these extreme values are to be avoided. A standard choice is the 4th-order B-splines, hence it is the value taken in this work. We remark however that the method is independent on our choice. The number of poles is determined empirically after carrying out computer simulations for different values and selecting the one with the best fitting error. Alternatively, a penalty term (e.g., the Akaike information criterion) can be inserted in Eq. (10) to penalize unnecessarily large values for this parameter.

Once these values are set, the memetic ICSA method is executed for an initial population of $\mathcal{P}$ individuals (nests). Each host nest, denoted by $\mathcal{N}_\kappa$ ($\kappa = 1, \ldots, \mathcal{P}$) and representing a potential solution of Eq. (10), is given by a vector:

$$\mathcal{N}_\kappa = \left(\xi_2^\kappa, \xi_3^\kappa, \ldots, \xi_{\chi-1}^\kappa; \upsilon_1^\kappa, \upsilon_2^\kappa, \ldots, \upsilon_\nu^\kappa; \Xi_0^\kappa, \Xi_1^\kappa, \ldots, \Xi_\sigma^\kappa\right) \tag{11}$$

corresponding to the data parameterization $\left\{\xi_2^\kappa, \xi_3^\kappa, \ldots, \xi_{\chi-1}^\kappa\right\} \in [0,1]^{\chi-1}$ the breakpoints $\{\upsilon_1^\kappa, \upsilon_2^\kappa, \ldots, \upsilon_\nu^\kappa\} \subset (0,1)$ and the poles $\{\Xi_0^\kappa, \Xi_1^\kappa, \ldots, \Xi_\sigma^\kappa\} \in \mathbb{R}^\sigma$, respectively. These vectors are initialized randomly within their respective domains and then sorted. The, our method is applied for a given number of generations $\mathcal{N}_{gen}$, large enough to

guarantee convergence. At each generation, our method obtains new potential solutions of the fitting problem. Some of them will improve the fitness and will be preserved for the next generation, while those with worse fitness will be discarded and replaced by new solutions. The nest with the best global value after convergence is the optimal solution of our problem.

4.3. Parameter tuning

A great shortcoming of nature-inspired metaheuristic optimization techniques is their dependence on several parameters that require proper tuning for good performance. This problem is exacerbated by the lack of sufficient theoretical results about optimal parameter values and the fact that such values do depend on the problem, so favorable values for a certain problem might become troublesome for other problems. This means that the parameter tuning is a serious issue when we apply metaheuristic techniques. Fortunately, our method is particularly well suited for this problem. In contrast to most metaheuristic methods, our approach requires only three parameters:

- the number of generations, $\mathcal{N}_{gen}$,
- the size of our population, $\mathcal{P}$, and
- the probability p_a.

Finding proper values for these parameters is a fully empirical task. Based on hundreds of executions, we found that $\mathcal{N}_{iter} = 20,000$ is enough to reach convergence for most examples of our benchmark. However, the examples with the largest amount of feature points might require as many as $30,000$ generations for optimality. We also tested population sizes ranging from 50 to 200 individuals, and found that $\mathcal{P} = 100$ is adequate for our problem. Finally, we tested values of p_a from 0.1 to 0.9 with step-size 0.05 and found little variation in our results, although values in the range $0.1 - 0.4$ perform slightly better. We eventually set $p_a = 0.3$ in this paper.

4.4. Implementation issues

The source code of our method has been implemented by the authors in *Matlab*, version 2015b running on Windows 10 OS. Our implementation of the ICSA method is based on a very efficient vectorized implementation of the original CSA freely available in [33], but adapted to the improved version as described in [41]. Our implementation of the local search procedure is based on [30] but strongly optimized for better performance. The experiments were executed on a 3.7 GHz. Intel Core i7 processor PC with 16 GB. of RAM.

5. Computational Experiments

5.1. Benchmark and Results

We applied our method to several examples of macroscopic images of skin lesions. In this paper, we restrict the discussion to a benchmark of ten medical images, labelled

from Example I to Example X and shown in Figure 1. All images have been obtained from the repository of digital medical images of the Department of Dermatology of the Medical Center, Groningen University (The Netherlands). All images correspond to melanoma except Examples I, III and IV, which correspond to benign skin lesions (naveus in all cases). As shown in Figure 1, it is very difficult to distinguish visually the melanoma from other skin lesions.

Only two examples of our benchmark (Examples II and IV) are graphically displayed to keep the manuscript in manageable size. They are shown in Figs. 2 and 3, respectively. Both figures share a similar structure: they show the original skin lesion image (top-left), the best border curve obtained with our method along with the original and the recovered feature points (top-right), the lesion borderline from the feature points combined with the lesion image for better visualization (bottom-left) and the convergence diagram (bottom-right). From the figures we can see that our memetic ICSA method yields an excellent matching of the feature points for both examples. This fact is clearly noticeable in the top-right pictures, where the original feature points (shown as red empty circles) and the approximated lesion border curve (in blue solid line with filled diamond symbols for the corresponding recovered feature points) are displayed. Note the remarkable visual matching between the original and the recovered feature points for both examples. Similarly, good visual results have also been obtained for the other eight examples in the benchmark.

This very good visual matching is numerically confirmed by our results, reported in Table 2. The table shows the number of original feature points (second column) and the RMSE (root-mean-square error) obtained with our method (last column) for ten examples in the benchmark, arranged in rows. The RMSE error is given by: $RMSE = \sqrt{\Lambda/\chi}$ and is preferred over the Λ value because the later does not consider the number of feature points. As shown in last column of the table, the RMSE takes values between low 10^{-1} and high 10^{-2}, which means a very good fitting error in all cases. We remark that these error values also depend on the quality of feature points, which are obtained manually and hence, subjected to noise. In other words, the process does not rely exclusively on the efficiency of the method, with the quality of initial screening by the dermatologist also being an important factor. Obviously, it would be desirable to develop an automatic procedure for this initial screening as well, but this task is out of the scope of this paper.

5.2. Comparative Analysis

It is always convenient to carry out a comparison between our method and other alternative approaches in the field. For this comparative work, we consider three types of methods: on one hand, we consider the classical mathematical procedures for B-spline curves given by three standard parameterization techniques (uniform, chord-length, and centripetal) and two methods for computing the breakpoints (uniform and averaging), as described in [11, 37]. The combination of all couples parameterization-breakpoints gives a total of six methods. They are shown in columns 3-5 of the table, where each column shows (in rows) the results of the uniform (U) and averaging (A) breakpoint computation methods for each parameterization scheme. We also con-

sider two of the most popular state-of-the-art approaches in the medical imaging field: thresholding [39] and clustering [6]. The corresponding RMSE errors are reported in columns 6–7 of Table 2. Finally, we include in this discussion the results obtained with our previous cukoo search algorithm method for Bézier curves reported in our conference paper in [19] (column 8) and the results of the ICSA method with B-spline curves without the local search, i.e., the non-memetic version of our method (column 9). Finally, the RMSE results with our memetic ICSA method for B-spline curves are shown in column 10. For each example, the best results are boldfaced for easier identification.

The results of this comparative analysis show that our new method outperforms the ten alternative methods used in our comparison for the examples in our benchmark. In particular, this new method improves the results of our previous conference paper (column 8) even although it was also based on the cuckoo search algorithm. This fact can be attributed to three factors: on one hand, to the ability of the B-splines to approximate the feature points better than the Bézier curves owing to the extra degrees of freedom given by the breakpoints and the use of a low degree for the curve, in good agreement with the reviewers comments; on other hand, to the use of an improved version of the cuckoo search algorithm; and, finally, to the hybridization with an effective local search algorithm. The effect of this last factor becomes evident from the comparison between the last two columns in Table 2. On the other hand, our method improves the results of the thresholding and clustering methods, which are widely considered two of the best state-of-the-art techniques in medical imaging. Note, for instance, that these methods improve the results with the standard CSA in our conference paper for the Examples VI, VII, IX and X. However, they are in turn outperformed by the method in this paper for all instances in our benchmark.

6. Conclusions and Future Work

This work is a substantial extension of a previous conference paper at Cyberworlds 2018 for automatic border detection of cutaneous melanoma and other skin lesions from macroscopic medical images. Using a set of feature points obtained by a dermatologist and laying on the boundary of the skin lesion, the paper introduces a new method to compute automatically the B-spline curve fitting such feature points better according to the least-squares approximation. The method is based on an improved version of the cuckoo search algorithm in which the parameters are allowed to change dynamically over the generations. This scheme is hybridized with the Luus-Jaakola local search heuristics for better performance. Experimental results on a benchmark of ten medical images of skin lesions (mostly melanomas) show that our method performs very well and yields a border curve enclosing the lesion and fitting the feature points with high accuracy. A comparative analysis with ten alternative methods in the literature (including six standard mathematical methods for B-spline fitting, two state-of-the art approaches in medical imaging, the previous method in our conference paper and the non-memetic version of our method) shows that our method outperforms all these methods in terms of numerical accuracy for all instances in our benchmark.

Of course, the method also comes with limitations. In our opinion, the most critical one is the computation time. Although the CPU time depends on the particular example under analysis and many other factors, our simulations require typically about 20,000 iterations or more to converge, which means several minutes for an individual execution. This fact prevents the method to be applied to real-time diagnosis or other medical applications where computational speed is a critical factor. We remark, however, that these CPU times are still quite competitive with those of state-of-the-art approaches in the field.

Regarding the future work, our method is sensitive to the quality of the feature points, which are acquired by manual procedures. To overcome this limitation, we plan to analyze some interesting approaches based on fusion thresholding [1] to capture the feature points automatically, so that our method is seamlessly integrated in a fully automatic pipeline. Possible modifications of our method to decrease its computation time are also part of our goals for future work in this field.

References

[1] Q. Abbas, M. E. Celebi, I. F. Garcia, M. Rashid: Lesion Border Detection in Dermoscopy Images Using Dynamic Programming, *Skin Research and Technology*, **17**(1), 91–100 (2011).

[2] A.A. Abbas, X. Guo, W.H. Tan, H.A. Jalab: Combined Spline and B-spline for an Improved Automatic Skin Lesion Segmentation in Dermoscopic Images Using Optimal Color Channel. *Journal of Medical Systems*, **38**, 80–80 (2014).

[3] G. Argenziano, H.P. Soyer, V. De Giorgi: *Dermoscopy: A Tutorial*. EDRA Medical Publishing & New Media (2002).

[4] Barhak, J., Fischer, A.: Parameterization and reconstruction from 3D scattered points based on neural network and PDE techniques. *IEEE Trans. on Visualization and Computer Graphics*, **7**(1) (2001) 1-16.

[5] Barnhill, R.E.: *Geometric Processing for Design and Manufacturing*. SIAM, Philadelphia (1992).

[6] M. E. Celebi, H. Iyatomi, G. Schaefer, W. V. Stoecker: Lesion Border Detection in Dermoscopy Images. *Computerized Medical Imaging and Graphics*, **33**(2), 148–153 (2009).

[7] De Jong, K.A.: *Evolutionary Computation: A Unified Approach*. MIT Press, Cambridge MA (2006).

[8] Dierckx, P.: *Curve and Surface Fitting with Splines*. Oxford University Press, Oxford (1993).

[9] Engelbretch, A.P.: *Fundamentals of Computational Swarm Intelligence*. John Wiley and Sons, Chichester, England (2005).

[10] B. Erkol, R. H. Moss, R. J. Stanley, W. V. Stoecker, E. Hvatum: Automatic Lesion Boundary Detection in Dermoscopy Images Using Gradient Vector Flow Snakes. *Skin Research and Technology*, **11**(1), 17–26 (2005).

[11] Farin, G.: *Curves and surfaces for CAGD (5th ed.).* Morgan Kaufmann, San Francisco (2002).

[12] Gálvez, A., Iglesias A.: Efficient particle swarm optimization approach for data fitting with free knot B-splines. *Computer-Aided Design*, **43**(12) (2011) 1683-1692.

[13] Gálvez A., Iglesias A.: Firefly algorithm for explicit B-Spline curve fitting to data points. *Mathematical Problems in Engineering*, (2013) Article ID 528215, 12 pages.

[14] Gálvez A., Iglesias A.: From nonlinear optimization to convex optimization through firefly algorithm and indirect approach with applications to CAD/CAM. *The Scientific World Journal*, (2013) Article ID 283919, 10 pages.

[15] Gálvez A., Iglesias A.: New memetic self-adaptive firefly algorithm for continuous optimization. *International Journal of Bio-Inspired Computation*, 8(5), 300–317 (2016).

[16] Gálvez A., Iglesias A., Avila, A., Otero, C., Arias, R., Manchado, C.: Elitist clonal selection algorithm for optimal choice of free knots in B-spline data fitting. *Applied Soft Computing*, **26** (2015) 90-106.

[17] Gálvez, A., Iglesias, A., Cobo, A., Puig-Pey, J., Espinola, J.: Bézier curve and surface fitting of 3D point clouds through genetic algorithms, functional networks and least-squares approximation. *Lectures Notes in Computer Science*, **4706** (2007) 680-693.

[18] Gálvez A., Iglesias A.: A new iterative mutually-coupled hybrid GA-PSO approach for curve fitting in manufacturing. *Applied Soft Computing*, **13**(3) (2013) 1491-1504.

[19] Gálvez A., Iglesias A.: Computational intelligence CSA-based approach for machine-driven calculation of outline curves of cutaneous melanoma. *Proc. of Cyberworlds 2018*, IEEE Computer Society Press, 270–275 (2018).

[20] R. Garnavi, M. Aldeen, M. E. Celebi, G. Varigos, S. Finch: Border Detection in Dermoscopy Images Using Hybrid Thresholding on Optimized Color Channels. *Computerized Medical Imaging and Graphics*, **35**(2), 105–115 (2011).

[21] Gu, P., Yan, X.: Neural network approach to the reconstruction of free-form surfaces for reverse engineering. *Computer-Aided Design* **27**(1) (1995) 59-64.

[22] Hoffmann, M.: Numerical control of Kohonen neural network for scattered data approximation. *Numerical Algorithms*, **39**, (2005) 175-186.

[23] Holland. J.H.: *Adaptation in Natural and Artificial Systems*. University of Michigan Press, Ann Arbor (1975).

[24] Iglesias, A., Echevarría, G., Gálvez, A.: Functional networks for B-spline surface reconstruction. *Future Generation Computer Systems*, **20**(8) (2004) 1337-1353.

[25] Jing, L., Sun, L.: Fitting B-spline curves by least squares support vector machines. In: *Proc. of the 2nd. Int. Conf. on Neural Networks & Brain*. Beijing (China). IEEE Press (2005) 905-909.

[26] Jupp, D.L.B.: Approximation to data by splines with free knots. *SIAM Journal of Numerical Analysis*, **15** (1978) 328-343.

[27] M. Kass, A. Witkin, D. Terzopoulos: Snakes: active contour models. International Journal of Computer Vision 1, 321–331 (1988s).

[28] Kennedy, J., Eberhart, R.C., Shi, Y.: *Swarm Intelligence*. Morgan Kaufmann Publishers, San Francisco (2001).

[29] Knopf, G.K., Kofman, J.: Adaptive reconstruction of free-form surfaces using Bernstein basis function networks. *Engineering Applications of Artificial Intelligence*, **14**(5) (2001) 577-588.

[30] Luus, R. Jaakola, T.H.I.: Optimization by direct search and systematic reduction of the size of search region. *American Institute of Chemical Engineers Journal (AIChE)*,**19**(4), 760–766 (1973).

[31] Z. Ma, J.M. Tavares: A novel approach to segment skin lesions in dermoscopic images based on a deformable model. *IEEE Journal of Biomedical and Health Informatics*, **20**, 615–623 (2016).

[32] D.A. Machado, G. Giraldi, A.A. Novotny: Multi-object segmentation approach based on topological derivative and level set method. *Integrated Computer-Aided Engineering*, **18**, 301–311 (2011).

[33] MatlabCentral repository: *http://www.mathworks.com/matlabcentral/fileexchange/29809-cuckoo-search-cs-algorithm* (last retrieved on May 6th 2018).

[34] Park, H.: An error-bounded approximate method for representing planar curves in B-splines. *Computer Aided Geometric Design* **21** (2004) 479-497.

[35] Park, H., Lee, J.H.: B-spline curve fitting based on adaptive curve refinement using dominant points. *Computer-Aided Design* **39** (2007) 439-451.

[36] Patrikalakis NM, Maekawa T. *Shape Interrogation for Computer Aided Design and Manufacturing*. Springer Verlag, Heidelberg: 2002.

[37] Piegl L, Tiller W. The NURBS Book. Springer Verlag, Berlin Heidelberg: 1997.

[38] P. Schmid: Segmentation of Digitized Dermatoscopic Images by Two-Dimensional Color Clustering. *IEEE Transactions on Medical Imaging*, **18**(2), 164–171 (1999).

[39] Sezgin, M., Sankur, B.: Survey over image thresholding techniques and quantitative performance evaluation. *Journal of Electronic Imaging*, **13**, 146–165 (2004).

[40] Ulker, E., Arslan, A.: Automatic knot adjustment using an artificial immune system for B-spline curve approximation. *Information Sciences*, **179** (2009) 1483-1494.

[41] Valian, E., Tavakoli, S., Mohanna, S., Hahgi, A.: Improved cuckoo search for reliability optimization problems. *Computers & Industrial Engineering*, **64**, 459–468 (2013).

[42] Wang, W.P., Pottmann, H., Liu, Y.: Fitting B-spline curves to point clouds by curvature-based squared distance minimization. *ACM Transactions on Graphics*, **25**(2) (2006) 214-238.

[43] Yang, X.-S.: *Nature-Inspired Metaheuristic Algorithms (2nd. Edition)*. Luniver Press, Frome, UK (2010).

[44] Yang, X.-S.: *Engineering Optimization: An Introduction with Metaheuristic Applications*. Wiley & Sons, New Jersey (2010).

[45] Yang, X.S., Deb, S.: Cuckoo search via Lévy flights. In: *Proc. World Congress on Nature & Biologically Inspired Computing (NaBIC)*. IEEE (2009) 210-214.

[46] Yang, X.S., Deb, S.: Engineering optimization by cuckoo search. *Int. J. Mathematical Modelling and Numerical Optimization*, **1**(4) (2010) 330-343.

[47] Yoshimoto, F., Moriyama, M., Harada, T.: Automatic knot adjustment by a genetic algorithm for data fitting with a spline. *Proc. of Shape Modeling International'99*, IEEE Computer Society Press (1999) 162-169.

[48] Yoshimoto, F., Harada T., Yoshimoto, Y.: Data fitting with a spline using a real-coded algorithm. *Computer-Aided Design*, **35** (2003) 751-760.

[49] H. Zhou, G. Schaefer, A. Sadka, M. E. Celebi: Anisotropic Mean Shift Based Fuzzy C-Means Segmentation of Dermoscopy Images. *IEEE Journal of Selected Topics in Signal Processing*, **3**(1) 26–34 (2009).

[50] H. Zhou, G. Schaefer, M. E. Celebi, F. Lin, T. Liu: Gradient Vector Flow with Mean Shift for Skin Lesion Segmentation. *Computerized Medical Imaging and Graphics*, **35**(2), 121–127 (2011).

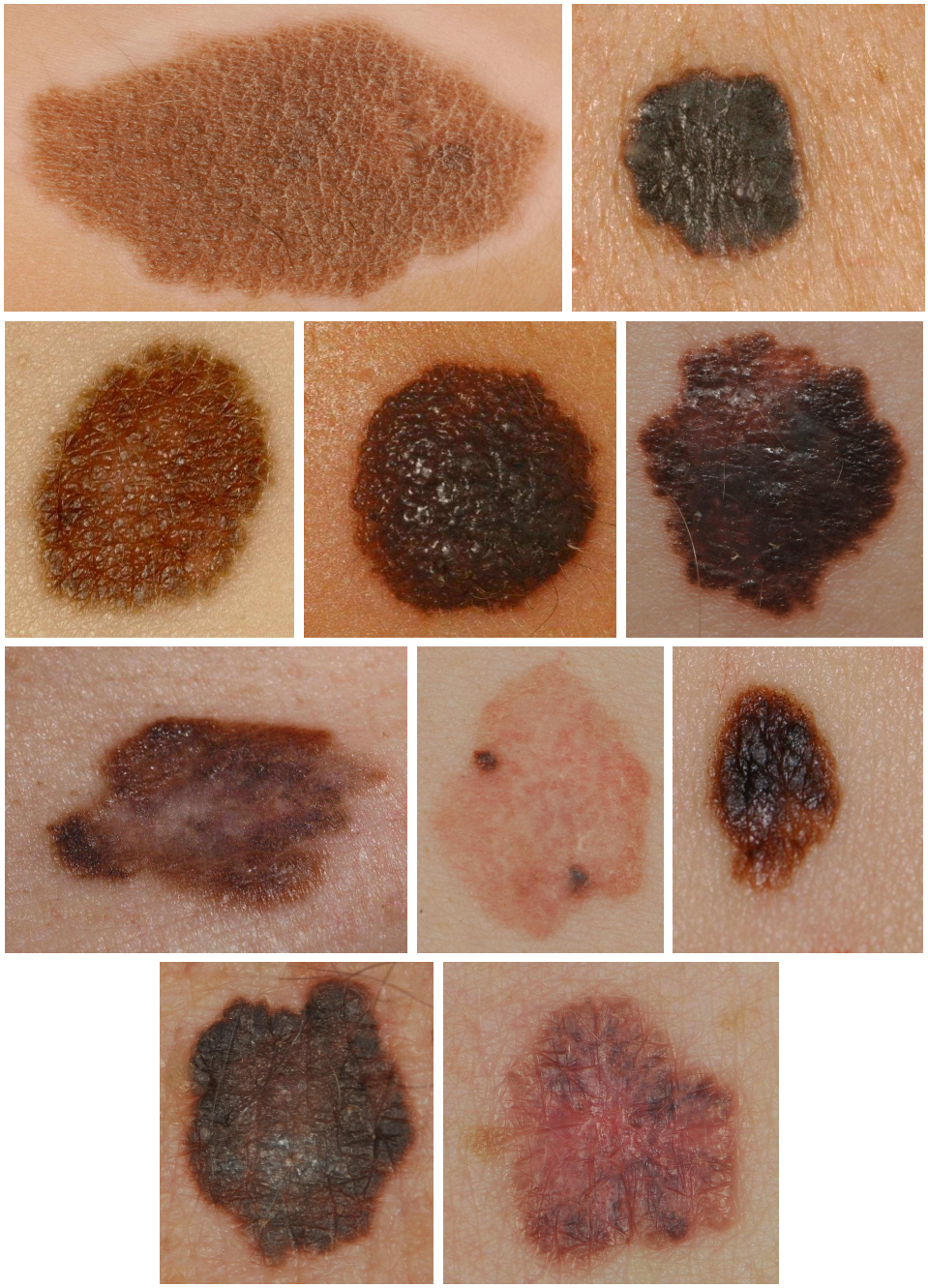

Figure 1: Benchmark of skin lesion images used in this paper: (l-r, t-b) Examples I to X.

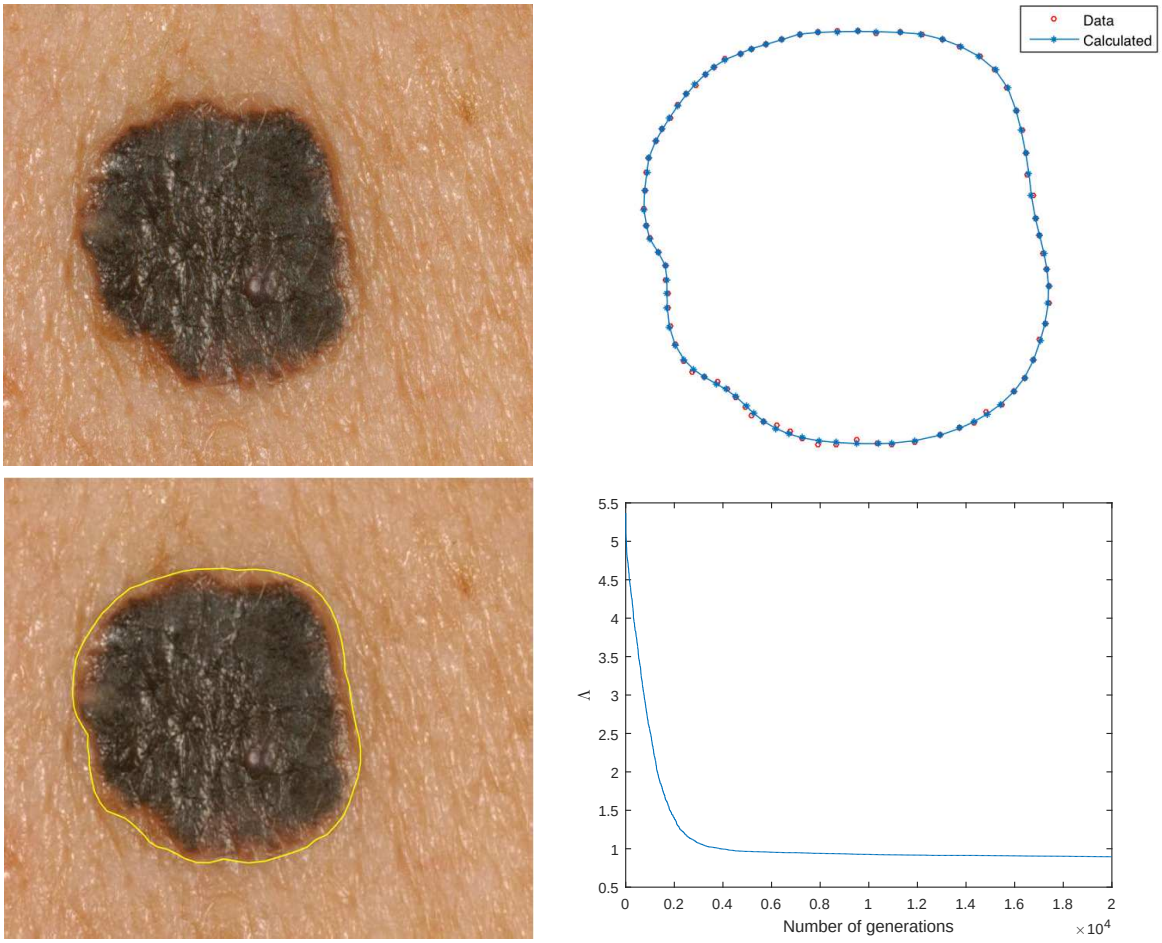

Figure 2: Example II (melanoma): (top-left) lesion image; (top-right) best border curve with original and recovered feature points; (bottom-left) lesion borderline from feature points superimposed on the lesion image for better visualization; (bottom-right) convergence diagram of our method.

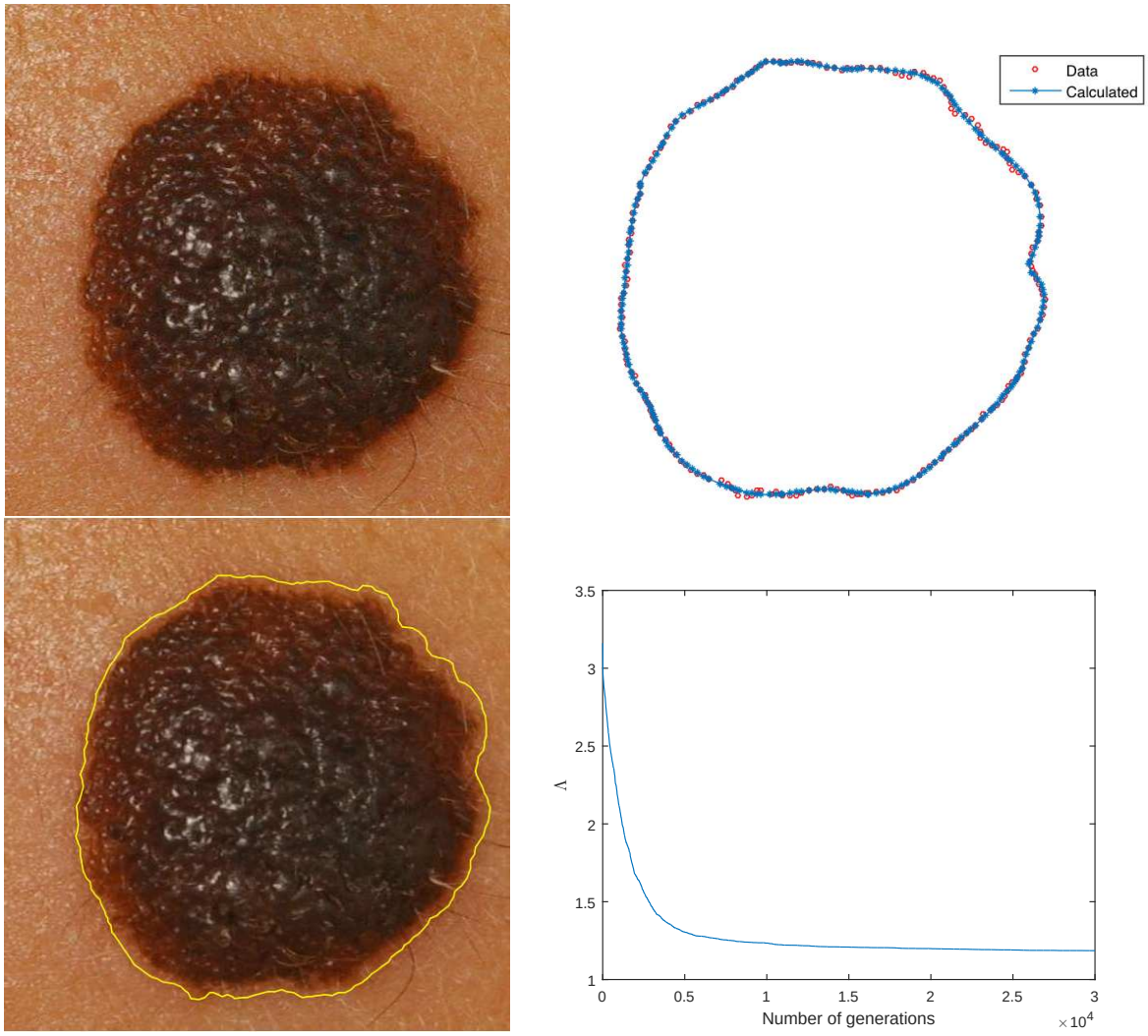

Figure 3: Example IV (naveus): (top-left) lesion image; (top-right) best border curve with original and recovered feature points; (bottom-left) lesion borderline from feature points superimposed on the lesion image for better visualization; (bottom-right) convergence diagram of our method.

Table 2: Comparative results of our method with ten alternative methods in the literature (in columns) for the instances in our benchmark (in rows). From left to right: example, number of feature points, classical mathematical techniques for parameterization (uniform, chord-length and centripetal) and breakpoints (in rows: uniform (U) and averaging (A)), state-of-the-art approaches (thresholding, clustering), the previous CSA method in [19], the improved cuckoo search method (ICSA) without local search, and the memetic ICSA (the method introduced in this paper).

Example	*# points*	*Uniform*	*Chord-length*	*Centripetal*	*Thresholding*	*Clustering*	*CSA*	*ICSA*	*Memetic ICSA*
I	223	3.2918E−1 (U) 3.1126E−1 (A)	3.0223E−1 (U) 2.6871E−1 (A)	2.9806E−1 (U) 2.7133E−1 (A)	2.1615E−1	1.9739E−1	1.5674E−1	1.4375E−1	**1.2912E−1**
II	77	2.3525E−1 (U) 2.1996E−1 (A)	2.0219E−1 (U) 1.7828E−1 (A)	1.9832E−1 (U) 17651E−1 (A)	1.6318E−1	1.5494E−1	1.2594E−1	9.9217E−2	**9.8654E−2**
III	162	3.6322E−1 (U) 3.4911E−1 (A)	2.9177E−1 (U) 2.7314E−1 (A)	2.8351E−1 (U) 2.6502E−1 (A)	2.1166E−1	2.1397E−1	1.0321E−1	8.8773E−2	**8.7355E−2**
IV	220	3.4592E−1 (U) 3.0973E−1 (A)	2.5924E−1 (U) 2.3691E−1 (A)	2.6102E−1 (U) 2.4015E−1 (A)	2.1358E−1	2.0709E−1	9.0672E−2	8.2656E−2	**8.0493E−2**
V	149	4.3651E−1 (U) 4.1908E−1 (A)	4.0547E−1 (U) 3.6925E−1 (A)	3.9833E−1 (U) 3.7442E−1 (A)	3.6815E−1	3.7626E−1	1.4777E−1	1.1150E−1	**1.0603E−1**
VI	213	3.7615E−1 (U) 3.5908E−1 (A)	3.4423E−1 (U) 3.2112E−1 (A)	3.4681E−1 (U) 3.1788E−1 (A)	3.1244E−1	2.9275E−1	3.2166E−1	2.8996E−1	**2.8315E−1**
VII	96	1.6013E−1 (U) 1.2956E−1 (A)	1.2814E−1 (U) 9.6644E−2 (A)	1.3207E−1 (U) 9.9167E−2 (A)	9.2512E−2	9.2753E−2	1.0422E−1	7.9113E−2	**7.8086E−2**
VIII	113	3.0392E−1 (U) 2.8752E−1 (A)	2.6322E−1 (U) 2.4215E−1 (A)	2.6019E−1 (U) 2.4533E−1 (A)	2.3907E−1	2.4449E−1	2.3827E−1	2.1224E−1	**2.0578E−1**
IX	162	2.9667E−1 (U) 2.8702E−1 (A)	2.5291E−1 (U) 2.3723E−1 (A)	2.5488E−1 (U) 2.4259E−1 (A)	2.2904E−1	2.5306E−1	2.3116E−1	2.1635E−1	**2.1104E−1**
X	155	2.4893E−1 (U) 2.3726E−1 (A)	2.1133E−1 (U) 1.9675E−1 (A)	2.0426E−1 (U) 1.8506E−1 (A)	1.8609E−1	1.8214E−1	1.8375E−1	1.5108E−1	**1.4492E−1**